Molecular Biology of the Cell
Vol. 19, 5347–5359, December 2008

Isoform and Splice-Variant Specific Functions of Dynamin-2 Revealed by Analysis of Conditional Knock-Out Cells

Ya-Wen Liu, Mark C. Surka, Thomas Schroeter, Vasyl Lukiyanchuk, and Sandra L. Schmid

Department of Cell Biology, The Scripps Research Institute, La Jolla, CA 92037

Submitted August 29, 2008; Revised October 1, 2008; Accepted October 3, 2008
Monitoring Editor: David G. Drubin

Dynamin (Dyn) is a multifunctional GTPase implicated in several cellular events, including endocytosis, intracellular trafficking, cell signaling, and cytokinesis. The mammalian genome encodes three isoforms, Dyn1, Dyn2, and Dyn3, and several splice variants of each, leading to the suggestion that distinct isoforms and/or distinct splice variants might mediate distinct cellular functions. We generated a conditional Dyn2 KO cell line and performed knockout and reconstitution experiments to explore the isoform- and splice variant specific cellular functions of ubiquitously expressed Dyn2. We find that Dyn2 is required for clathrin-mediated endocytosis (CME), p75 export from the Golgi, and PDGF-stimulated macropinocytosis and cytokinesis, but not for other endocytic pathways. Surprisingly, CME and p75 exocytosis were efficiently rescued by reintroduction of Dyn2, but not Dyn1, suggesting that these two isoforms function differentially in vesicular trafficking in nonneuronal cells. Both isoforms rescued macropinocytosis and cytokinesis, suggesting that dynamin function in these processes might be mechanistically distinct from its role in CME. Although all four Dyn2 splice variants could equally restore CME, Dyn2ba and -bb were more effective at restoring p75 exocytosis. This splice variant specificity correlated with their differential targeting to the Golgi. These studies reveal isoform and splice-variant specific functions for Dyn2.

INTRODUCTION

Dynamin (Dyn) is an ~100-kDa multidomain GTPase that was first identified as a microtubule binding and bundling protein (Shpetner and Vallee, 1989). Subsequently, dynamin was found to be the mammalian homologue of the *Drosophila* protein shibire, mutations in which block endocytosis, including synaptic vesicle recycling (Chen *et al.*, 1991; van der Bliek and Meyerowitz, 1991). Dynamin is conserved throughout higher eukaryotes. There is a single gene in *Drosophila* and *Caenorhabditis elegans*, but there are three dynamin isoforms in mammals: Dyn1, which is specifically expressed in neurons; Dyn2, which is ubiquitously expressed; and Dyn3, which is mainly expressed in the brain and testes (Urrutia *et al.*, 1997, Ferguson *et al.*, 2007).

The best-studied cellular function of dynamin is its involvement in clathrin-mediated endocytosis (CME; Hinshaw, 2000; Sever *et al.*, 2000; Praefcke and McMahon, 2004). However, dynamin has also been implicated in several other membrane-trafficking events including both caveolae-mediated and clathrin- and caveolin-independent endocytic pathways (Henley *et al.*, 1998; Oh *et al.*, 1998; Lamaze *et al.*, 2001; Pelkmans *et al.*, 2002), phagocytosis (Gold *et al.*, 1999; Yu *et al.*, 2006), macropinocytosis (Schlunck *et al.*, 2004), and trafficking from the *trans*-Golgi network (TGN; Jones *et al.*, 1998; Kreitzer *et al.*, 2000; Bonazzi *et al.*, 2005). Because these functions have mostly emerged from studying the effects of overexpression of dominant-negative dynamin mutants, they may reflect indirect or nonspecific effects. Moreover, it is not known whether different dynamin isoforms and/or splice variants participate in distinct membrane-trafficking events (McNiven *et al.*, 2000).

Recent studies have also implicated dynamin in cellular processes other than membrane trafficking. For example, dynamin may play significant roles in regulating actin assembly and reorganization via its interactions with many actin-binding proteins (Orth and McNiven, 2003; Schafer, 2004; Itoh *et al.*, 2005; Kruchten and McNiven, 2006). Dyn2, but not Dyn1 can function as a signaling GTPase to trigger p53-dependent apoptosis (Fish *et al.*, 2000). Interestingly, this signaling activity does not require dynamin's ability to self-assemble into the collar-like structures linked to membrane fission in CME (Soulet *et al.*, 2006). Moreover, analysis of Dyn2/Dyn1 chimeras has shown that Dyn2's signaling activity is conferred by its GTPase domain, despite its high degree of sequence identity with Dyn1. It has also been suggested that dynamin plays a role in cytokinesis (Konopka *et al.*, 2006). Dynamin mutations prevent cleavage furrow completion in *Drosophila* embryos and small interfering RNA (siRNA)-mediated knockdown causes a cytokinesis defect in *C. elegans*. Dyn2 has been localized to the centrosome and its knockdown has been suggested to cause a centrosome cohesion defect in mammalian cells (Thompson *et al.*, 2002; Konopka *et al.*, 2006). The mechanisms guiding these diverse dynamin-mediated processes remain to be established.

The multiple cellular functions that have been reported for dynamins would suggest that the different dynamin isoforms and/or splice variants might have different specific functions (McNiven *et al.*, 2000). However, because dynamin is a tetramer (Hinshaw and Schmid, 1995; Ramachandran *et al.*, 2007), overexpression of dominant-negative mutants—

This article was published online ahead of print in *MBC in Press* (http://www.molbiolcell.org/cgi/doi/10.1091/mbc.E08–08–0890) on October 15, 2008.

Address correspondence to: Sandra L. Schmid (slschmid@scripps.edu).

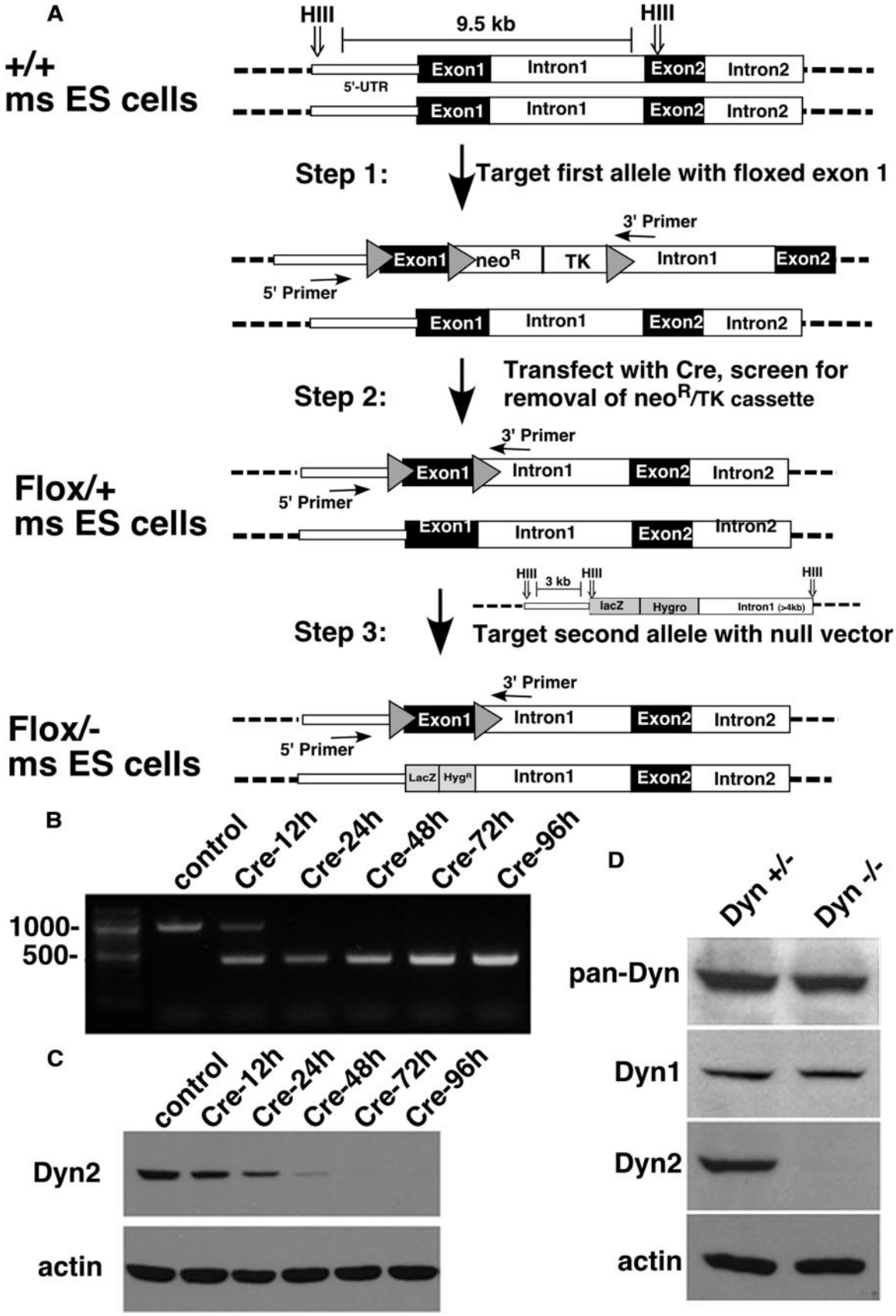

Figure 1. Generation of Dyn2 conditional KO cells. (A) Schematic diagram of the three-step strategy for generating $Dyn2^{flox}/-$ ES cells, by sequential transfection and selection of mouse ES cells with a conditional null vector and subsequent transfection and selection with a second

the approach most commonly taken to study dynamin function in vivo—might not distinguish subtle isoform and splice variant differences due to the formation of heterotetramers and nonselective dominant interference of all endogenous dynamin isoforms. Therefore, to identify isoform- and/or splice-variant–specific functions of dynamin, it would be necessary to perform isoform-specific knockout and reconstitution experiments. In support of this approach, it was recently shown (Ferguson *et al.*, 2007) that Dyn1 KO synapses exhibited a less severe phenotype than obtained with dominant-negative dynamin mutants, such as shibire (Koenig and Ikeda, 1989) or with the dynamin inhibitor, dynasore (Newton *et al.*, 2006). These authors also provided evidence for isoform-specific function at the synapse because reexpression of either Dyn1 or Dyn3, but only to a lesser degree by Dyn2, could rescue the defect in Dyn1 KO neurons (Ferguson *et al.*, 2007).

Here we report the generation and characterization of a Dyn2 conditional KO fibroblastoid cell line that has allowed us to define isoform and splice-variant specific functions of the ubiquitously expressed dynamin isoform.

MATERIALS AND METHODS

Generation of Dyn2^{flox}/null Conditional KO Embryonic Stem Cells

We generated a neomycin-resistant targeting vector in which loxP sites flank exon 1 of the Dyn2 gene. Briefly, a loxP site was inserted after the 5′ UTR region of the Dyn2 gene, and a loxP-flanked neomycin resistance (Neo^R) and thymidine kinase (TK) cassette was inserted into intron 1. The linearized vector was transfected into mouse embryonic stem (ES) cells, and neomycin-resistant clones were collected and assayed for proper gene insertion through PCR and Southern blotting techniques (Figure 1A, step 1). Neomycin-resistant ES clones were then transiently transfected with a vector encoding Cre recombinase to excise the Neo^R and TK cassette. TK negative clones were selected and then analyzed by PCR and Southern blotting to ensure that the correct transposition event had occurred, i.e., that only the Neo^R and TK genes were excised, leaving behind a loxP-flanked exon 1 of Dyn2, and thus generating Dyn2^{flox}/+ ES cells (Figure 1A, step 2). To knock out the remaining wild-type allele, a linearized KO vector, in which the majority of exon 1 of Dyn2 was replaced by a LacZ-hygromycin resistance (Hyg^R) cassette, was transfected into the Dyn2^{flox}/+ ES cell clone, and hygromycin-resistant clones were selected (Figure 1A, step 3). PCR analysis was used to screen for clones that had correctly inserted the Dyn2 KO vector into the WT Dyn2 allele, generating Dyn2^{flox}/− ES cells.

Differentiation and Immortalization of Dyn2^{flox}/− ES cells

Maintenance and growth of the Dyn2^{flox}/− ES cells was performed as previously described (Conner, 2001). Differentiation of the Dyn2^{flox}/− ES cells involved growth of the ES cells in suspension for 5 d, giving rise to embryoid bodies (EBs). The EBs were then subsequently plated on adherent tissue culture dishes, and differentiation and growth continued in the presence of DMEM with high glucose (4500 mg/l), 2 mM L-glutamine, and sodium pyruvate, containing 10% (vol/vol) FCS (Hyclone, Logan, UT), 1× MEM nonessential amino acids (from 100× stock), and 20 mM HEPES, pH 7.3. Passage of the adherent cells continued for four passage cycles, and immortalization was performed.

Dyn2^{flox}/− cells were immortalized by infection with amphotropic retroviruses harboring the large T antigen from SV40 (kindly given by Peiqing Sun, The Scripps Research Institute). Clones of fibroblastoid-like cells were then generated after immortalization. These fibroblastoid Dyn2^{flox}/− cells were maintained in MEM with 10% FCS for no more than 30 passages. To excise exon 1, the cells were infected with adenovirus expressing Cre recombinase (Vector Biolaboratories, Burlingame, CA).

Figure 1 (cont). null targeting vector. (B) PCR analysis of the Dyn2 KO cells after Cre adenovirus infection. DNA isolated at the indicated times after Cre adenovirus infection was used as a template to amplify the exon 1 region of Dyn2 to monitor excision efficiency (primer positions indicated in A). (C) Dyn2 protein depletion. Cell lysates were harvested at the indicated times after Cre adenovirus infection and Western-blotted with anti-Dyn2 or actin antibodies. (D) Dynamin expression in the Dyn2^{flox}/− ES cells. Cell lysates from control or Cre adenovirus–infected cells were harvested 96 h after infection and blotted with anti-pan-dynamin or with the indicated isoform-specific antibodies.

Antibodies

Anti-Dyn1 antibody (ab3456) was purchased from Abcam (Cambridge, MA) and anti-Dyn2 antibody (sc-6400) was from Santa Cruz Biotechnology (Santa Cruz, CA). Anti-β-tubulin antibody (T-4026) was from Sigma (St. Louis, MO) and anti-actin antibody (MAB1501R) was from Chemicon International (Temecula, CA). Anti-Dyn3 polyclonal serum was generously provided by S. Ferguson and P. De Camilli (Yale) because we found that the commercially available anti-Dyn3 antibody (Abcam, ab3458) recognized a nonspecific band of 100 kDa in all of our cell lysates. The rabbit anti-pan-dynamin (748) was generated in our lab and hemagglutinin (HA; 12CA5) antibodies were purified from hybridomas obtained from Ian Wilson (TSRI).

Retroviral Transduction and Fluorescence-activated Cell Sorting

HA-tagged human Dyn1 (ba) or rat Dyn2 (aa, ab, ba, and bb) were cloned into the retrovirus vector pMIEG3 containing an internal ribosome entry site allowing expression of enhanced green fluorescent protein (MIEG3-EGFP; Yang *et al.*, 2006). Alternatively, HA-Dyn1 (ba) or HA-Dyn2 (ba) were fused to GFP on their C-termini and used to generate retroviruses. Retroviral supernatant was prepared by using the Phoenix packaging cell system, and subsequent infection was carried out in the presence of 8 μg/ml Polybrene (Sigma) according to the described protocols (Guo and Zheng, 2004). Cells were harvested 48 h after infection and GFP-positive cells with low expression levels were isolated using fluorescence-activated cell sorting (FACS).

Cell Cycle Distribution Analysis

Analysis of cell cycle distribution was determined by propidium iodide (PI) staining and flow cytometry. Cells were harvested by trypsinization and 70% cold ethanol fixation overnight. Cells were then washed in PBS and resuspended in PBS containing 10 μg/ml PI and 250 μg/ml RNase A. Cells were incubated at 37°C for 1 h before flow cytometric analysis. Histograms of the PI signal were obtained using FlowJo software (Tree Star, Ashland, OR).

Adenovirus Infection

Cells were coinfected with adenovirus expressing the tetracycline regulatable transactivator (tTA) and adenovirus encoding either HA-Dyn1K44A or HA-Dyn2K44A under control of a tetracycline-regulatable promoter as previous described (Fish *et al.*, 2000). Control cells were infected only with the tTA-adenovirus. Endocytosis assays were performed ~24 h after infection.

Genotype and Protein Expression Analysis

To analyze the knockout efficiency of Cre adenovirus infection, total cellular DNA was isolated with DNeasy Blood and Tissue kit (QIAGEN, Chatsworth, CA), and the region of Dyn2 exon 1 was amplified with the primer pair: Dyn2-3515, CAGGTTGACGTTTCTGCGACCATTA, and Dyn2-4369, CAGCCATAGCCGGAACTAGAAGCAC (as Figure 1A indicates) in PCR. To analyze protein expression, lysates were obtained from cells after different times of Cre adenoviral infection and analyzed by Western blotting using anti-Dyn2 antibodies or anti-pan dynamin antibodies as indicated.

Endocytosis Assay

Transferrin internalization were performed as described (van der Bliek *et al.*, 1993) using biotinylated transferrin (Tfn) as ligand and assessing its internalization into an avidin-inaccessible compartment. For cholera toxin B (CTB) uptake, cells on coverslips were incubated with 1 μg/ml Alexa fluor-594 CTB (Invitrogen, Carlsbad, CA) for 30 min at 4°C and then shifted to 37°C medium to allow internalization. Cells were washed extensively with cold PBS and acid buffer (150 mM NaCl, 150 mM glycine, pH 2.0) and then fixed and mounted for fluorescence microscopy. Internalization of lactosylceramide (LacCer) was analyzed as described in Antonescu *et al.* (2008) with some modification. Briefly, cells on coverslips were washed with cold PBS++ (PBS with 1 mM $CaCl_2$ and 1 mM $MgCl_2$) and incubated with 5 μg/ml BODIPY FL C_5-LacCer (Molecular Probes, Eugene, OR) in PBS++ for 1 h at 4°C. After washing off unbound LacCer with ice-cold PBS+, cells were incubated with warm media for 5 min at 37°C and then arrested with two washes of ice-cold PBS++. LacCer remaining at the cell surface was then removed by six 10-min washes in 2% (wt/vol) defatted BSA (Sigma) at 10°C. After fixation and mounting, the cells were viewed under an epi-fluorescence microscope.

To analyze macropinocytosis, cells were starved in 0.2% serum for 16 h and then incubated with 1 mg/ml HRP with or without 10 ng/ml PDGF for 10 min in 37°C. The uptake was stopped by transferring to 4°C, and cells were washed six times with cold PBS++ containing 0.2% BSA. Cells were trypsinized, harvested, and lysed. Then the cleared lysate was assayed for enzyme activity and protein concentration.

p75 TGN Export Assay

The TGN-exit assay of p75-mRFP (from E. Rodriguez-Boulan, Weill Medical College of Cornell University, New York, NY) was performed as described (Bonazzi *et al.*, 2005) with some modification. Briefly, the cells transfected with p75-monermeric red fluorescent protein (mRFP) were incubated overnight in complete medium. To accumulate p75-mRPF in the TGN and deplete newly synthesized p75-mRPF from the early secretory pathway, the cells were incubated 3.5 h at 20°C in bicarbonate-free medium and 0.5 h under the same condition with 100 μg/ml cycloheximide. To monitor p75 exit from the TGN, the temperature was shifted to 32°C, and the samples were fixed with 4% paraformaldehyde at the indicated time.

Microscopy

For indirect immunofluorescence staining, cells cultured overnight on polylysine–coated coverslips were fixed for 40 min with 4% paraformaldehyde and permeabilized with 0.05% saponin. After blocking with 2% BSA, cells were stained with either anti-HA or anti-β- tubulin antibodies. To detect actin, after 5 min PDGF or mock treatment and PBS wash, cells were fixed, permeabilized, and stained with Alexa Fluor 568-phalloidin (Invitrogen).

For Dyn1 and -2 localization, cells expressing either GFP-tagged dynamin or HA-tagged dynamin were fixed and permeabilized simultaneously with 2% warm paraformaldehyde and 0.5% Triton X-100 for 2 min, to reduce cytosolic background staining, and then fixed with 4% paraformaldehyde for 40 min. After immunofluorescence staining or mounting alone, cells were observed under wide-field epifluorescence microscopy using an inverted Olympus IX-70 microscope (Melville, NY).

RESULTS

Dyn2 Conditional KO Cells

To better define Dyn2-specific cellular functions and to establish cell lines for reconstitution experiments, we generated a conditional null Dyn2 cell line. To this end, a floxed allele of Dyn2 was designed and used to generate $Dyn2^{flox}/-$ ES cells by three sequential transfections and selections (Figure 1A), as described in detail in *Materials and Methods.* Cells were first selected for incorporation of the conditional targeting vector, and then they were transfected with Cre recombinase and screened for excision of the Neo/TK sequences. The resulting $Dyn2^{flox}/+$ cells were then transfected with a nonconditional KO targeting vector to disrupt the remaining wild-type allele and selected to obtain $Dyn2^{flox}/-$ cells. The genotypes at each stage were confirmed by PCR and Southern blot analysis (data not shown). These $Dyn2^{flox}/-$ cells were then used to generate immortalized, fibroblastoid cells by in vitro differentiation of embryoid bodies and infection with retroviruses harboring the SV40 large T antigen.

Infection of the $Dyn2^{flox}/-$ cells with commercially available adenoviruses encoding Cre recombinase resulted in complete excision of Dyn2 exon 1 within 24 h, as detected by PCR (Figure 1B). Dyn2 protein levels were undetectable by 72 h after infection (Figure 1C). Unexpectedly, despite a complete knockdown of endogenous Dyn2, total dynamin in these cells, detected using a pan-dynamin antibody, was reduced by <50% (Figure 1D). Using isoform-specific antibodies, we confirmed that these cells express both Dyn1 and -2, but not -3 (data not shown) and that Dyn1 expression was

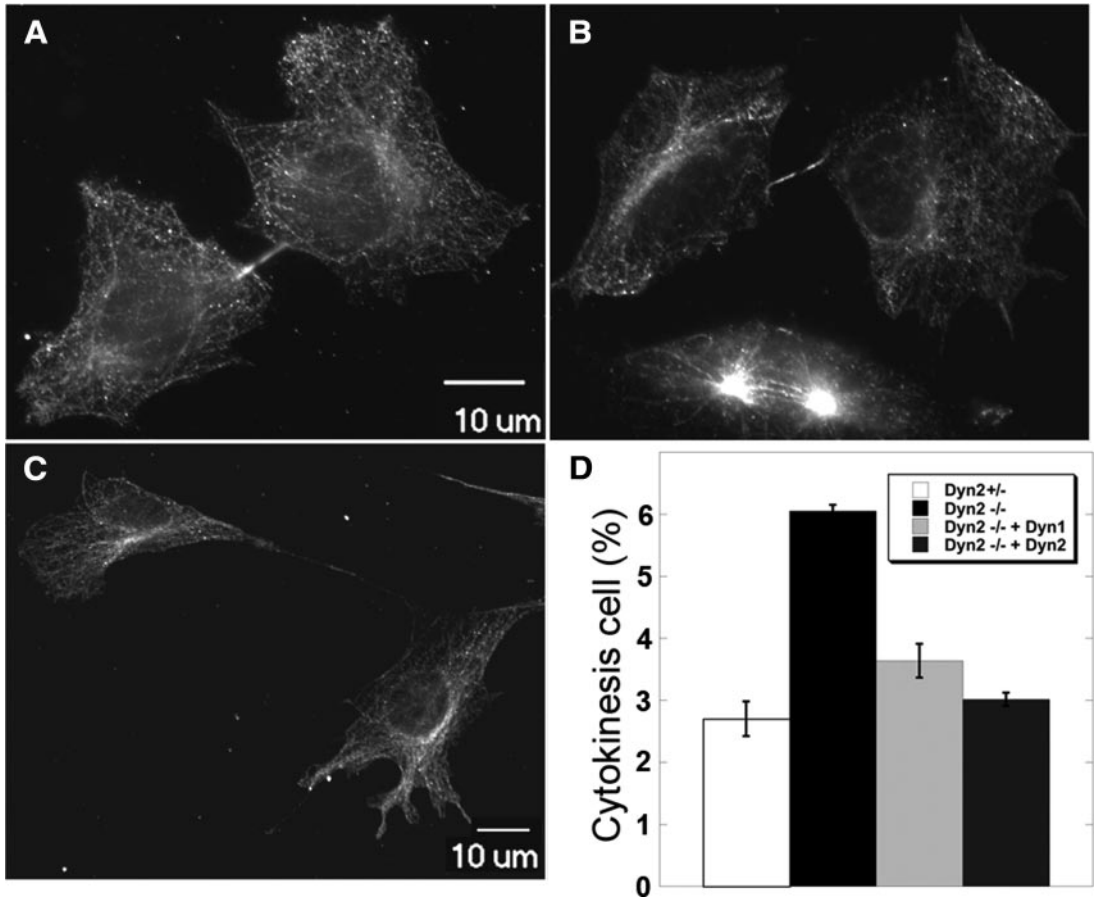

Figure 2. Cytokinesis defect in Dyn2 KO cells. $Dyn2^{flox}/-$ (A) or Dyn2 KO cells (B and C) were fixed and stained with anti-β-tubulin antibody to detect the midbody and the morphology of cells undergoing cytokinesis. Panels A and B are same scale, and C is a lower scale image to detect the long connection between two incompletely separated cells. (D) Quantitation of percentage of control, Dyn2 KO cells or Dyn2 KO cells reconstituted with either Dyn2 or -1, accumulating in late cytokinesis, based on detection of midbody staining. Error bars, SD of three independent experiments; 300 cells for each experiment were scored and counted.

unaffected by knockdown of Dyn2. As an aside, we found that most cells in culture, including COS-1, HeLa, HEK293, and BSC-1 cells also express both Dyn1 and -2 to varying degrees (see Supplemental Figure S1), indicating that the tissue-specific expression seen in whole animals can be lost in culture.

Dyn2 KO Cells Exhibit Growth and Cytokinesis Defects

Dyn2 has been reported to function in chromosome cohesion (Thompson *et al.,* 2004) and in cytokinesis (Thompson *et al.,* 2002), and indeed we found that after excision of Dyn2 by Cre recombinase, the cells (hereafter referred to as Dyn2 KO cells) grew more slowly than the control ($Dyn2^{flox}/-$) cells (Supplemental Figure S2A). PI staining and flow cytometric analysis of the DNA content did not reveal a specific defect in cell cycle progression (Supplemental Figure S2B), nor did we detect an increase in the percentage of multinucleate cells by DAPI staining (data not shown). We also did not detect an increase in apoptosis. However, given the strong evidence for a role for dynamin in cytokinesis in *C. elegans* and other organisms (Konopka *et al.,* 2006), we used real-time imaging to monitor cell division in control and Dyn2 KO cells (Supplemental Movies S1 and S2). Consistent with the DNA content analysis, both control and KO cells progressed through mitosis, from prophase to telophase, with similar kinetics (23.00 ± 13.08 and 24.00 ± 6.00 min, respectively). However, the time required for completion of the midbody separation in KO cells was significantly longer than in control cells. Compared with an average of 54 min for cytokinesis in control cells, even after 2.5 h of imaging, many Dyn2 KO cells still had not completed cytokinesis. Given the delay in midbody scission, we used immunofluorescence staining of β-tubulin to detect midbodies in control (Figure 2A) and Dyn2 KO cells (Figure 2, B and C), as an assay for this late cytokinesis defect. As expected, we found that the percentage of Dyn2 KO cells with detectable midbodies was higher than in control cells (Figure 2D). We also detected examples in which daughter Dyn2 KO cells were connected with long membrane tethers consistent with a late block in cytokinesis and suggesting that adherent daughter cells might complete cytokinesis as they migrate away from each other (Figure 2, B and C).

These results are consistent with evidence that dynamin functions in cytokinesis in *Drosophila* and *C. elegans* (Konopka *et al.,* 2006); however, these organisms express only a single dynamin gene. We therefore wondered whether cytokinesis represented an isoform-specific function of the ubiquitously expressed Dyn2. To test this possibility we generated retroviruses encoding HA-Dyn1 and HA-Dyn2 using a retroviral vector containing an internal ribosomal entry site (IRES) upstream of GFP according to the strategy of Yang *et al.* (2006). We used FACS to select GFP-expressing cells that also expressed low, near endogenous levels of HA-dynamin (see below). After Cre adenovirus infection and KO of endogenous Dyn2, cells reconstituted with either Dyn1 or -2 displayed growth rates similar to control cells (Supplemental Figure S2A) and also showed reduced accumulation of midbody staining (Figure 2D). These data establish a role for mammalian dynamin in cytokinesis and suggest, perhaps unexpectedly, that either Dyn1 or -2 isoforms can fulfill this function.

Dyn2 Is Specifically Required for Clathrin-mediated Endocytosis in Fibroblastoid Cells

Overexpression studies have suggested that Dyn1 and -2 also play functionally redundant roles in clathrin-mediated endocytosis (Altschuler *et al.,* 1998). Therefore, given the partial knockdown of total dynamin in these cells, we did not expect to see a strong defect in CME. However, CME of Tfn was inhibited by ~80% in Dyn2 KO cells (Figure 3A), more than we would expect based on the proportional reduction of total dynamin. Moreover, overexpression of the dominant-negative Dyn1K44A mutant only slightly increased the level of inhibition of Tfn uptake (Figure 3B), indicating that the residual Tfn uptake in Dyn2 KO cells was both dynamin- and clathrin-independent. These data suggest that CME in these nonneuronal cells is preferentially dependent on Dyn2 compared with Dyn1.

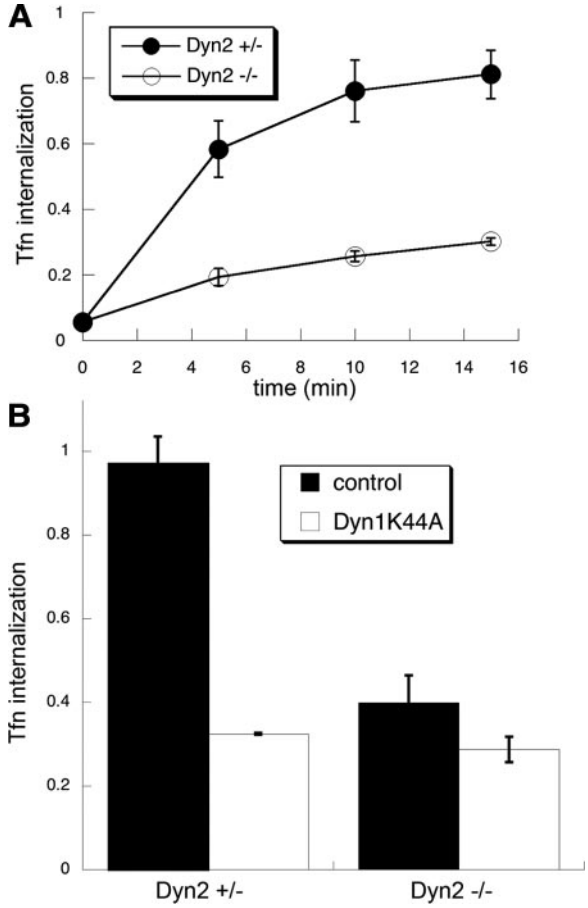

Figure 3. CME is potently inhibited in Dyn2 KO cells. (A) Kinetics of Tfn internalization in control and Dyn2 KO cells. Biotin-Tfn was incubated with $Dyn2^{flox}/-$ or Dyn2 KO cells for the indicated times at 37°C. Cells were returned to ice and internalized Tfn was detected as described in *Materials and Methods.* (B) Effects of Dyn1K44A overexpression on Tfn uptake in control and Dyn2 KO cells. $Dyn2^{flox}/-$ and Dyn2 KO cells were infected overnight with tTA-adenovirus alone (control) or together with Dyn1K44A-adenovirus. The extent of Tfn uptake after a 10-min incubation at 37°C was measured as described in *Materials and Methods.*

To directly test this hypothesis, we measured Tfn uptake in $Dyn2^{flox}/-$ cells that had been reconstituted with either HA-Dyn1 or HA-Dyn2 using retroviral IRES GFP vectors described above. After Cre adenovirus infection and KO of endogenous Dyn2, cells reconstituted with HA-Dyn2 exhibited fully restored Tfn endocytosis, whereas cells expressing HA-Dyn1 (Figure 4A) showed only partial recovery, despite exhibiting higher overall levels of dynamin expression (Figure 4A, right, lanes 3 and 4) and despite the ability of Dyn1 to rescue the growth defect of Dyn2 KO cells (Supplemental

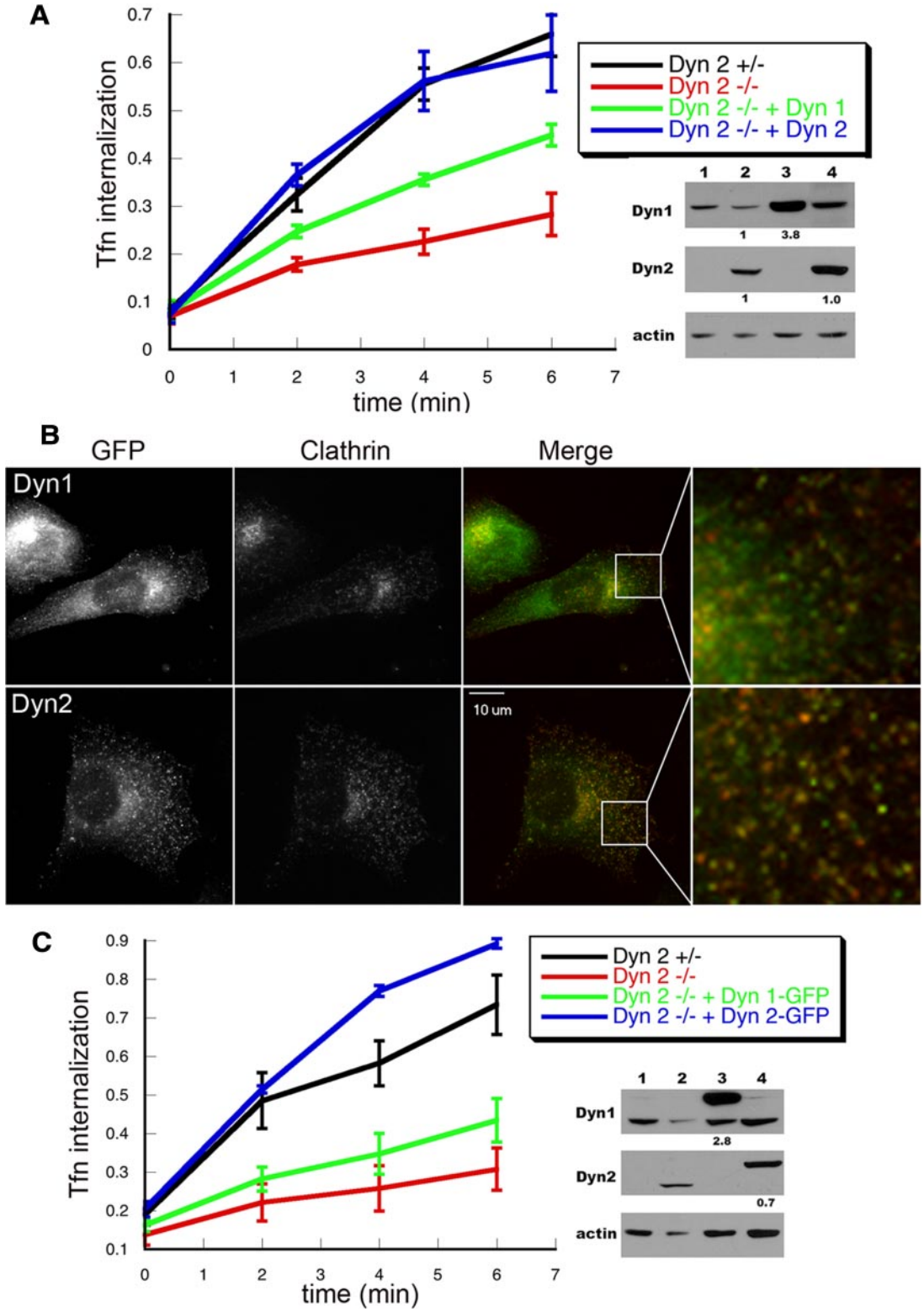

Figure 4. Dyn2 rescues CME in Dyn2 KO cells more efficiently than Dyn1. (A) Dyn2^{flox}/− cells were infected with retroviruses encoding HA-Dyn1 (ba) or HA-Dyn2 (ba) and IRES-driven GFP, FACS-sorted for comparable levels of expression, and subsequently infected with Cre adenovirus to delete endogenous Dyn2. Their ability to internalize Tfn was assessed relative to control and Dyn2 KO cells as described above. The accompanying gels are Western blots with the indicated antibodies showing relative levels of expression (lane 1, Dyn2 KO cells; lane 2, Control cells; lane 3, Dyn2 KO cells reconstituted with HA-Dyn1; lane 4, Dyn2 KO cells reconstituted with HA-Dyn2). The small numbers below lanes 3 and 4 in B and C are fold-expression relative to endogenous dynamin after normalizing to actin loading controls. (B and C) Dyn2^{flox}/− cells were infected with retroviruses encoding Dyn1 (ba)- or Dyn2 (ba)-GFP, FACS sorted for comparable levels of expression, and subsequently infected with Cre adenovirus to delete endogenous Dyn2. (B) Dyn2 KO cells expressing Dyn1-GFP or Dyn2-GFP and clathrin light chain-mCherry were fixed and observed under epi-fluorescence microscopy. (C) The kinetics of Tfn uptake in control, Dyn2 KO

Figure S2A). We also examined Tfn endocytosis in cells exhibiting even higher levels of overexpression and found that when Dyn1 was expressed at ~10 times higher than endogenous levels, it could restore the Tfn uptake defect in Dyn2 KO cells to 80–90% of control (data not shown).

Several groups have examined the dynamics of dynamin-GFP in live cells (Merrifield *et al.*, 2002; Soulet *et al.*, 2005) and some have reported differential behaviors of the two isoforms relative to clathrin-coated pit dynamics (Rappoport and Simon, 2003). To directly test the functionality of these C-terminally GFP-tagged constructs, we used retroviruses encoding either Dyn1-GFP or Dyn2-GFP to infect $Dyn2^{flox}/-$ cells and used FACS to select for cells expressing low or high levels of Dyn1-GFP or Dyn2-GFP. At high levels of overexpression, both Dyn1-GFP and Dyn2-GFP formed large aggregates in the cytosol (not shown). Therefore we restricted our analyses to cells expressing GFP-tagged proteins at levels near that of endogenous dynamin (Figure 4C, right). These cells were then infected with Cre adenovirus to knock out endogenous Dyn2. Both Dyn1-GFP and Dyn2-GFP were predominantly localized to the cytosol but could also be detected as punctate structures at the cell surface (Figure 4B). The colocalization of Dyn2-GFP with clathrin was greater than that of Dyn1-GFP (Figure 4B, right panels). We next examined Tfn uptake and found that the defect in CME could be fully rescued by Dyn2-GFP expression at near endogenous levels (Figure 4C). These data show that C-terminally tagged Dyn2 is fully functional (the slight increase over control cells most likely reflects small cell-to-cell variations). In contrast, and consistent with our analysis of untagged protein, Dyn1-GFP was only partially able to restore Tfn uptake (Figure 4C, right, lane 3 and 4).

Together, these data show that in these nonneuronal cells, Dyn2 is significantly more effective than Dyn1 in supporting CME.

Dyn2 Is Required for PDGF-stimulated Macropinocytosis, But Not for Other Endocytic Pathways

Multiple, mechanistically distinct endocytic pathways operate in mammalian cells (Conner and Schmid, 2003). To determine which of these might also specifically require Dyn2, we examined the uptake of other ligands and receptor classes. CTB is internalized by both caveolae-dependent and other raft-dependent endocytic pathways, which have been shown to be inhibited both by antibody microinjection and by overexpression of dominant negative dynamin mutants (Henley *et al.*, 1998; Oh *et al.*, 1998, Pelkmans *et al.*, 2002). We were unable to detect significant inhibition of CTB internalization in our Dyn2 KO cells (Figure 5A), although we confirmed findings of others that the overexpression of a dominant negative mutant Dyn2K44A blocks CTB uptake in our fibroblasts (Figure 5B). Similar results were obtained using BODIPY-LacCer, which is reported to be a more specific probe for caveolae-mediated endocytosis (Singh *et al.*, 2003; Figure 5C). Because overexpressed Dyn2K44A will dominantly interfere with the function of both endogenous Dyn2 and -1 isoforms, the more potent effect of dominant-negative overexpression suggests that the remaining Dyn1

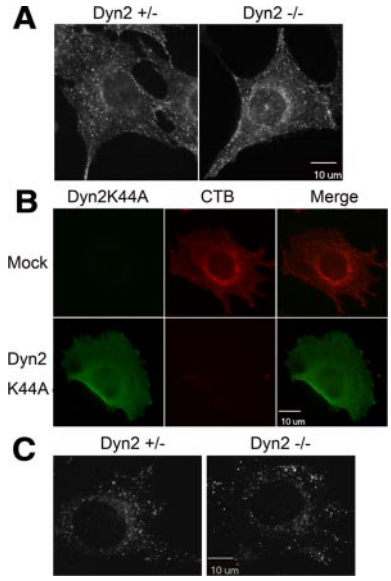

Figure 5. Dyn2 is not specifically required for cholera toxin, caveolae, or raft-mediated endocytosis. (A) Control and Dyn2 KO cells were incubated with Alexa fluor 594–conjugated cholera toxin B (CTB) for 5 min at 37°C. Surface-bound CTB was stripped by acid washing and internalized CTB detected by epifluorescence microscopy. (B) $Dyn2^{flox}/-$ cells were infected with Dyn2K44A or control adenovirus and then tested for CTB endocytosis as indicated in A. (C) BODIPY FL C_5-LacSer uptake. Five-minute internalization of BODIPY FL C_5-LacSer was analyzed in control and Dyn2 KO cells as described in *Materials and Methods.*

may be sufficient to support CTB uptake in the Dyn2 KO cells. Alternatively, the overexpressed Dyn2K44A may inhibit CTB uptake through indirect effects or by sequestering some other essential component. Regardless these results indicate that Dyn2 is not specifically required for CTB or caveolae endocytosis.

Recently, a clathrin- and caveolae-independent pathway that leads to the formation of GPI-anchored protein-enriched endosomal compartments (GEECs), has been identified. The GEEC pathway has been reported to be resistant to inhibition by dominant negative dynamin mutants (Sabharanjak *et al.*, 2002), and consistent with this, we found no detectable inhibition of uptake of rhodamine-conjugated folate by the endogenous GPI-anchored folate receptor in Dyn2 KO cells (Supplemental Figure S3).

The GEEC pathway has also been suggested to be responsible for the bulk of constitutive fluid phase endocytosis in mammalian cells (Kirkham *et al.*, 2005). Indeed, we found that constitutive fluid-phase endocytosis of HRP was not inhibited in Dyn2 KO cells (Figure 6A, serum-starved cells). Macropinocytosis, which is induced upon stimulation by growth factors, involves the actin-driven formation of membrane protrusions that engulf large volumes of fluids. There are conflicting reports as to a role for dynamin in macropinocytosis (Meier *et al.*, 2002; Schlunk *et al.*, 2004; Cao *et al.*, 2007). Macropinocytosis in our Dyn2 KO cells can be triggered by stimulation with PDGF, resulting in a transient, sixfold, increase in fluid phase uptake (Figure 6A, PDGF). This PDGF-stimulated increase in fluid phase endocytosis of HRP is partially inhibited in the Dyn2 KO cells to a degree that is roughly proportional to the extent of knockdown of total dynamin (i.e., ~50%). This suggests that both isoforms may function in PDGF-stimulated macropinocytosis and in-

Figure 4 (cont). cells and Dyn2 KO cells expressing Dyn2-GFP or Dyn1-GFP as indicated. The accompanying gels are Western blots with the indicated antibodies showing relative levels of expression (lane 1, Dyn2 KO cells; lane 2, Control cells; lane 3, Dyn2 KO cells reconstituted with Dyn1-GFP; lane 4, Dyn2 KO cells reconstituted with Dyn2-GFP).

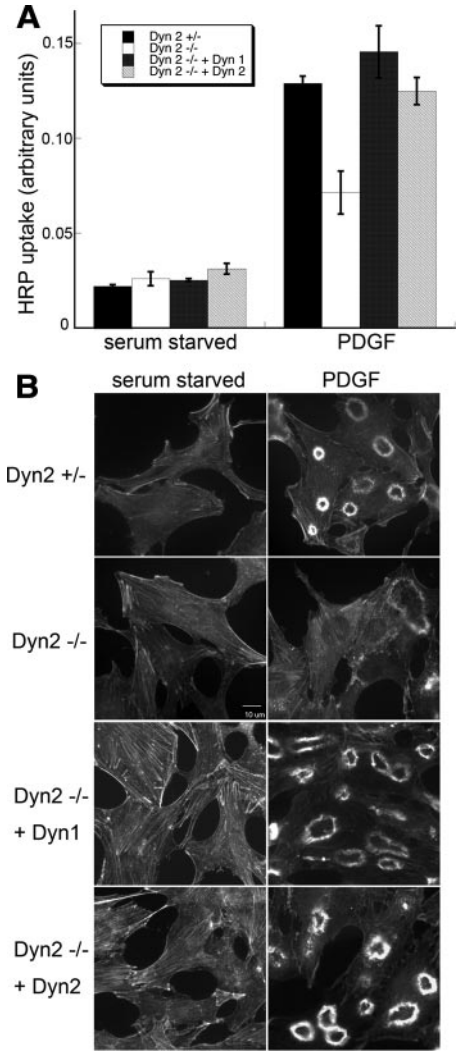

Figure 6. PDGF-stimulated macropinocytosis is supported by both Dyn1 and -2. (A) Fluid-phase uptake of HRP was measured in serum-starved cells before and after treatment with 10 ng/ml PDGF. Control and Dyn2 KO cells are equally effective at fluid-phase uptake under basal conditions, but Dyn2 KO cells are defective in PDGF-stimulated macropinocytosis. This defect is rescued by reexpression of either Dyn1 or -2. (B) Fluorescent phalloidin staining of actin in serum-starved and PDGF-treated cells reveals actin reorganization and dorsal ring formation upon PDGF stimulation. Dorsal ring formation is reduced in Dyn2 KO cells and restored by reintroduction of either Dyn1 or -2.

deed, reintroduction of either Dyn1 or -2 restores full activity in this assay (Figure 6A).

That either dynamin isoform can rescue PDGF-stimulated macropinocytosis distinguishes this activity of dynamin from its role in CME in these nonneuronal cells. Given that macropinocytosis is an actin-based process, it was possible that this activity reflected dynamin's function in regulating actin dynamics. To test this, we examined actin organization in control and PDGF-stimulated cells. There was no apparent change in actin stress fiber distribution in heterozygous control versus Dyn2 KO cells (Figure 6B). On stimulation with PDGF, a dramatic actin reorganization takes place as actin stress fibers disassemble and actin assembles to form membrane ruffles or dorsal rings (Figure 6B; see Supplemental Figure S4 for quantification). This actin reorganization is significantly diminished in Dyn2 KO cells (Figure 6B). As expected from our macropinocytosis assay results, both Dyn1 and -2 can restore PDGF-stimulated dorsal actin ring formation in Dyn2 KO cells. These data suggest that dynamin function in macropinocytosis might be related to its role in actin regulation and distinct from its role in CME. Indeed, as has been reported (Krueger *et al.*, 2003), Dyn2-GFP localizes to dorsal ruffles upon PDGF stimulation in punctate structures that do not colocalize with the clathrin-coated pits (Supplemental Figure S5).

Dyn2 Is Specifically Required for p75 Export from the TGN

There are conflicting reports as to whether dynamin plays a general role in transport of proteins from the TGN to the plasma membrane (Damke *et al.*, 1994; Altschuler *et al.*, 1998; Jones *et al.*, 1998; Kasai *et al.*, 1999), and more recent results suggest that dynamin's function in some TGN trafficking events might be cell-type specific (Bonazzi *et al.*, 2005). Nonetheless, there is a strong consensus for a requirement of Dyn2 in the export of the apical plasma membrane marker, p75/neurotrophin receptor, from the TGN (Kreitzer *et al.*, 2000; Bonazzi *et al.*, 2005). However, because these findings are based on overexpression of dominant-negative dynamin mutants, it is not known whether this represents an isoform-specific function of Dyn2. To test this we transfected Dyn2 KO cells with p75-mRFP overnight and then allowed newly synthesized protein to accumulate in the TGN by incubating cells for 4 h at 20°C. We then examined the efficiency of depletion of the TGN pool upon shift to 32°C. Whereas the accumulated p75-mRFP had left the TGN within 40 min in ~70% of heterozygous control cells, its export was severely impaired in Dyn2 KO cells (Figure 7, A and C). This defect was rescued upon reintroduction of Dyn2, but not Dyn1 (Figure 7, B and C). Thus, although both of these dynamin isoforms can localize to the Golgi compartment (Figure 4B), the export of p75 from the TGN appears to be another isoform-specific function of Dyn2.

A Specific Function for Dyn2 Splice Variants at the Golgi

Dyn2 has two alternatively spliced regions encoding sequences located within the middle domain that could result in four different splice variants, referred to as aa, ab, ba, and bb (Cao *et al.*, 1998; Figure 8A). Although all four splice variants of Dyn2 localize to clathrin-coated pits at the plasma membrane, it has been reported that Dyn2 splice variants carrying the second alternatively spliced 4-aa insert (Dyn2aa and Dyn2ba) also preferentially localize to the TGN (Cao *et al.*, 1998). These studies, however, involved Dyn2-GFP expression in cells also expressing endogenous Dyn2, thus complicating analysis of potential splice-variant specific functions due to heterotetramer formation with endogenous Dyn2. Indeed, coprecipitation studies showed that the exogenously expressed GFP-tagged dynamins could form hetero-oligomers with both endogenous Dyn1 and -2; however, at these low levels of exogenous dynamin expression, heteroligomers appeared to represent minor species compared with homo-oligomers (see Supplemental Figure S6). Nevertheless, to avoid possible complications due to heterooligomer formation between distinct Dyn2 splice variants, we separately introduced the various HA-Dyn2 splice variants into $Dyn2^{flox}/-$ cells using retroviral IRES GFP expression vectors, selected for low, near endogenous levels of HA-Dyn2 expression, and then deleted endogenous Dyn2 by Cre recombinase (Figure 8B). As previously reported, all four splice variants localized to punctate structures at the plasma membrane, but in contrast to previous findings, we

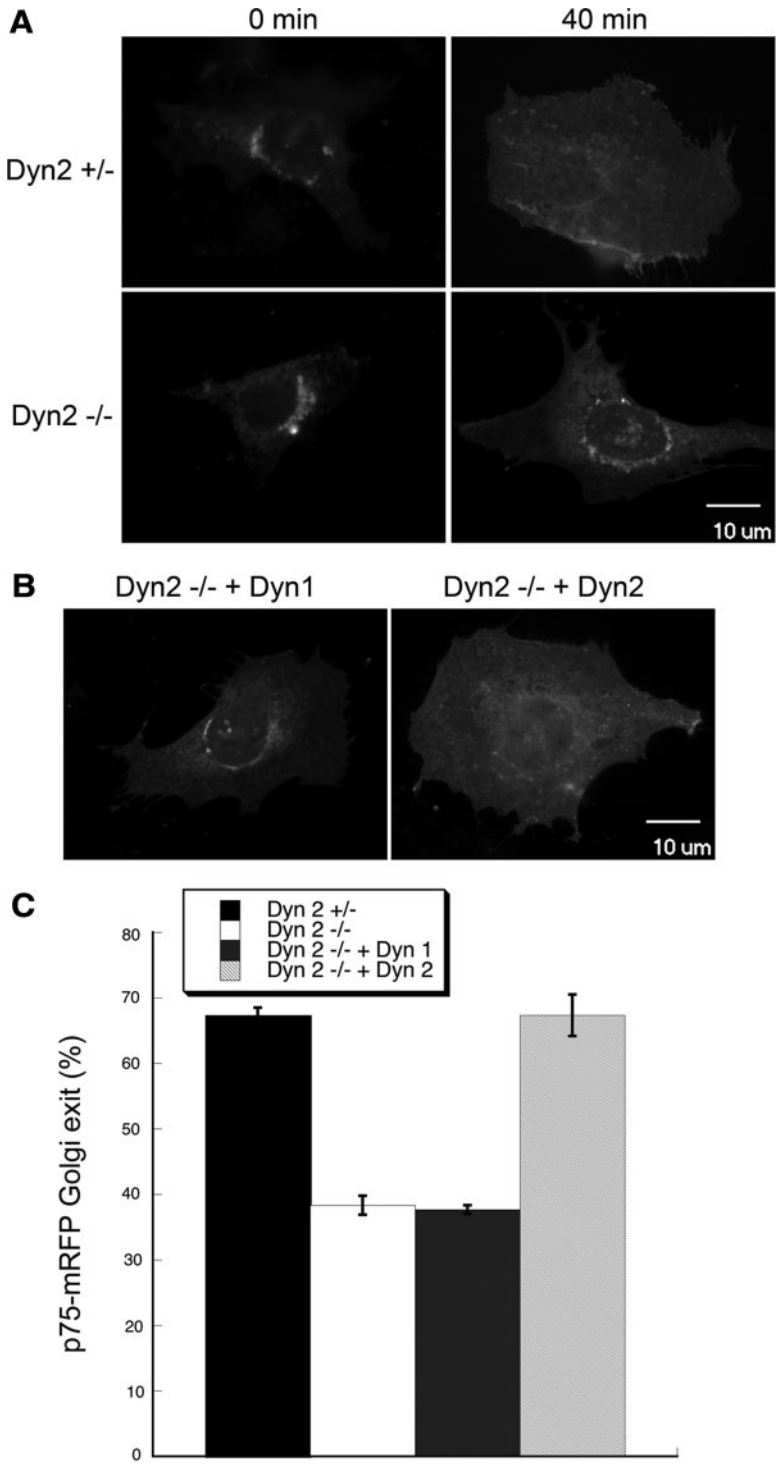

Figure 7. Dyn2 is specifically required for p75 export from the TGN. Control and Dyn2 KO cells were transfected with p75-mRFP/neurotropin receptor and at 24 h after infection, p75-mRFP was allowed to accumulate at the TGN as described in *Materials and Methods.* Cells were returned to 32°C to follow export of p75-mRFP from the TGN. (A) p75-mRFP accumulated in the TGN at t = 0 is largely depleted from the TGN at t = 40 min in control but not Dyn2 KO cells. (B) Reintroduction of Dyn2, but not Dyn1 can rescue p75-mRFP export in Dyn2 KO cells. (C) Quantification of p75-mRFP export in control, Dyn2 KO and Dyn1 or -2 reconstituted Dyn2 KO cells. The efficiency of p75-mRFP export from the TGN was determined by counting the percentage of cells without detectable p75-mRFP in the TGN. Three independent experiments and 100 cells for each experiment were scored and counted.

found that the two splice variants encoding the b variant of the first spliced region showed localization to the Golgi (Figure 8C). We performed PCR analysis of each cell line to confirm the splice variant of Dyn2 expressed (data not shown). Consistent with this localization, all four splice variants equally rescued the endocytosis defect in Dyn2 KO cells (Figure 8D), whereas Dyn2ba and Dyn2bb were more effective at rescuing p75 export from the TGN than Dyn2aa and Dyn2ab splice variants (Figure 8, E and F). Dyn1 also encodes two possible splice variants corresponding to aa 399-444 in its middle domain. The Dyn1 splice variant we used encodes residues that are most homologous to the b variant in Dyn2, consistent with its ability to localize to the Golgi. Hence its inability to rescue p75 export reflected a true isoform difference in function.

DISCUSSION

Dynamin 2, the ubiquitously expressed isoform of dynamin, has been implicated in diverse cellular functions, largely

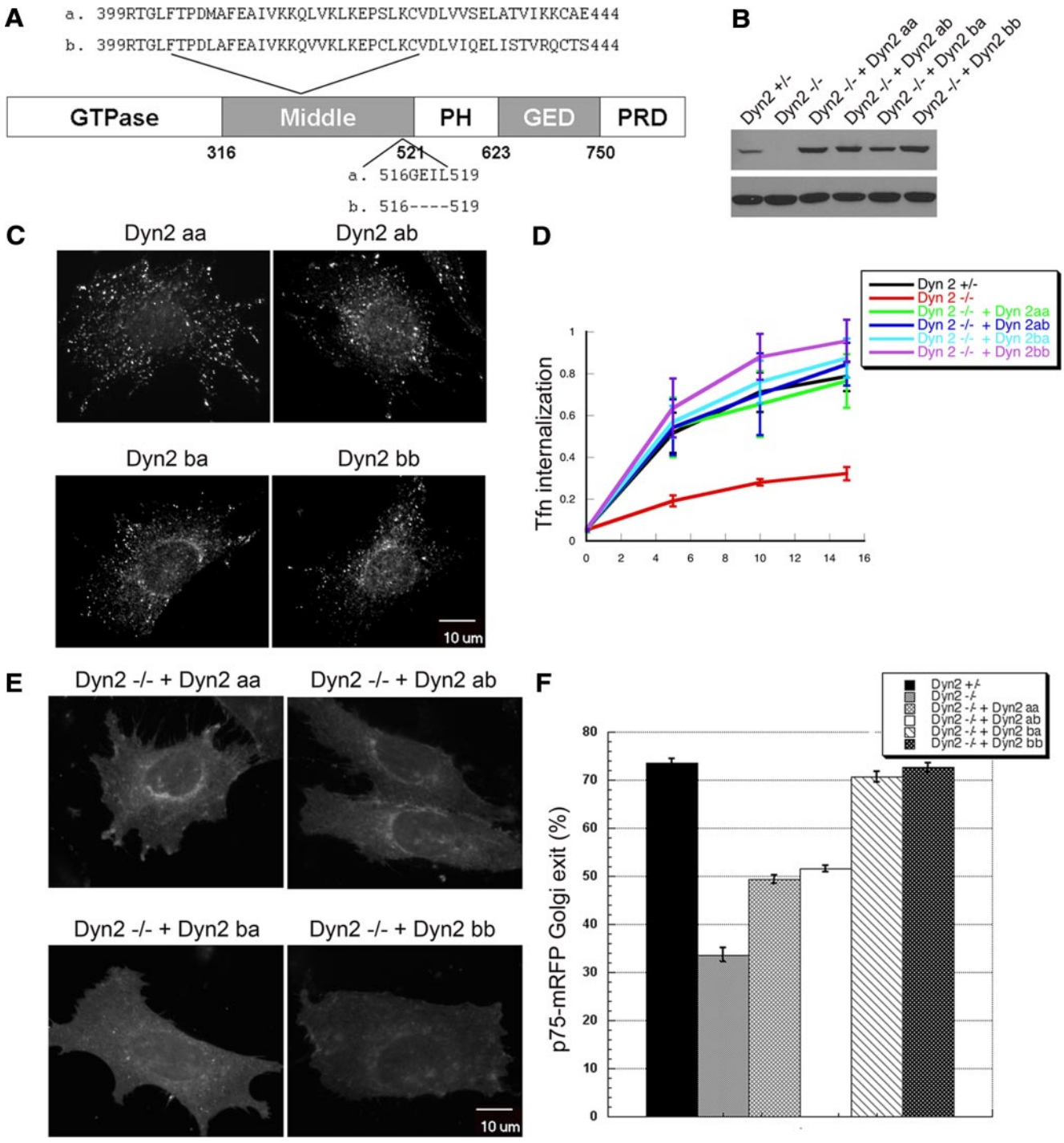

Figure 8. Dyn2 splice variants are specifically required for targeting and function at the Golgi. (A) Schematic and sequences of Dyn2 splice variants. (B) The HA-tagged Dyn2 aa, ab, ba, or bb splice variants were introduced into Dyn2 KO cells using IRES-GFP retrovirus vectors. Low expressing cells were selected by FACS sorting. Western blot using anti-Dyn2 antibody showing comparable expression levels of Dyn2 splice variants reintroduced into Dyn2 KO cells. (C) Localization of four Dyn2 splice variants. Four Dyn2 splice variants expressed in Dyn2 KO cells were detected using anti-HA antibody. (D) Tfn internalization was measured as described in *Materials and Methods*. All 4 Dyn2 splice variants function in CME. (E) Differential ability of Dyn2 splice variants to rescue p75-mRFP export from the TGN. (F) Quantification of the activity of different Dyn2 splice variants on p75-mRFP export. Three independent experiments as described in E were performed, and 100 cells from each experiment were scored for TGN exit of p75-mRFP.

through overexpression of dominant-negative mutants. In addition to the potential of nonspecific effects, this approach has the disadvantage of not being able to assess potential isoform or splice-variant specific functions. To overcome these problems, we have generated conditional Dyn2 KO cells and reintroduced specific isoforms and splice variants to investigate the specificity for dynamin requirements in these distinct cellular functions. The Dyn2^{flox}/− ES-derived

fibroblastoid cells we generated, like other cells in culture, have failed to maintain the tissue-specific regulation of dynamin isoform expression and therefore also express Dyn1. Although this is a disadvantage in identifying redundant functions of Dyn1 and -2, it has the advantage of enabling us to readily identify Dyn2-specific phenotypes and functions.

Perhaps the biggest surprise from these studies is our finding that clathrin-mediated endocytosis in these nonneuronal cells is preferentially supported by Dyn2 and is only weakly supported by Dyn1. This result, although unexpected, is complementary to findings from analysis of Dyn1 KO mice on isoform-specific functions of dynamin at the synapse (Ferguson *et al.,* 2007). These studies revealed that Dyn1 was specifically required for rapid synaptic vesicle recycling under conditions of intense stimulation, but was dispensable for synaptic vesicle recycling under steady-state conditions. Interestingly, neuronal Dyn3 redistributed to the synapse in Dyn1 KO mice, presumably to compensate for the loss of Dyn1 in mediating endocytosis and synaptic vesicle recycling, whereas Dyn2 remained diffusely distributed. Moreover, overexpression of Dyn1 or Dyn3 fully rescued the endocytosis defect in cultured Dyn1 KO neurons, whereas Dyn2 was much less effective. Similarly, others have reported that the rapid versus slow endocytic pathways trigger by stimulation of chromaffin cells are differentially sensitive to microinjected Dyn1 versus Dyn2 antibodies, respectively (Artelejo *et al.,* 2002). Thus, together these results suggest that the neuronal-specific Dyn1 and -3 isoforms have adapted to function during rapid stimulus-induced endocytosis, whereas Dyn2 has adapted to support constitutive CME in nonneuronal cells.

Dyn1 and -2 are 79% similar in their sequences and both are equally similar to the single dynamin isoforms in *Drosophila* and *C. elegans*. What might account for their differential ability to support CME in nonneuronal cells? We observed that Dyn2 colocalizes with endocytic coated pits to a greater extent than Dyn1; thus, this differential efficiency of targeting may contribute to their functional differences. However, studies with Dyn1-GFP have shown that it is recruited to clathrin-coated pits in nonneuronal cells before vesicle release (Merrifield *et al.,* 2002), and thus other factors must also contribute to this striking functional difference. We list three, not mutually exclusive, possibilities. First, the differential activities may reflect differences in their biochemical and enzymatic properties. Most biochemical analyses have focused on Dyn1; however, previous studies have shown that Dyn2 has a higher propensity for self-assembly compared with Dyn1 and may have a higher basal rate of GTP hydrolysis (Warnock *et al.,* 1997; Lin *et al.,* 1997). Interestingly, nonconserved residues in the PH domain have been shown to confer isoform-specific functions that distinguish Dyn1 and -2 activity in compensatory endocytosis in adrenal cells (Artelejo *et al.,* 1997). A more careful and thorough comparison of Dyn1 and -2 enzymatic activities and biochemical properties may reveal differences that account for their differing activities in CME. A second possibility is that Dyn1 and -2 interact differentially with different partner proteins. These partners could either differentially affect dynamin's biochemical properties or its intracellular targeting. Most dynamin partners interact with dynamin through its C-terminal proline/arginine domain (PRD). These domains are indeed the most divergent between the two isoforms, although they are both highly basic (pI $\geq$ 12) and proline rich (30%). Although most dynamin partners have been identified from analysis of brain lysates, to our knowledge when tested they have been shown to bind to both Dyn1 and -2. However, in light of our findings, it will be interesting to look for Dyn2-specific binding partners in nonneuronal cell lysates. A third possibility relates to differential regulation of the two dynamin isoforms by posttranslational modification (Cousin and Robinson, 2001). Both dynamin isoforms are known to be phosphorylated in vivo, and it may be that regulatory kinases and/or phosphatases necessary for Dyn1 function are not present or properly regulated in nonneuronal cells. Further experiments will be necessary to test these three possibilities.

As was observed for synaptic vesicle recycling, overexpression of dominant-negative dynamin mutants inhibited a broader set of endocytic pathways than did knockout of a single dynamin isoform. These data suggest that the remaining Dyn1 is functional in nonneuronal cells for mediating other forms of endocytosis that, for example, lead to CTB uptake. Dyn1 was also able to support PDGF-stimulated macropinocytosis as effectively as Dyn2. Thus, Dyn1 is not completely inactive in nonneuronal cells. From these data we can also infer that the mechanism for Dyn1 and -2 function in PDGF-stimulated macropinocytosis is distinct from the mechanism for Dyn2 function in CME.

There are conflicting results as to the requirement for dynamin in macropinocytosis. Others have reported that dominant-negative mutants of dynamin do not inhibit adenovirus-stimulated macropinocytosis (Meier *et al.,* 2002) or vaccinia-virus induced macropinocytosis (Mercer and Helenius, 2008) and that microinjection of Dyn2 antibodies or siRNA depletion of Dyn2 does not inhibit EGF-stimulated macropinocytosis (Cao *et al.,* 2007). In contrast, and consistent with our findings, overexpression of dominant-negative Dyn2 was previously shown to inhibit PDGF-stimulated macropinocytosis in Rat1 cells (Schlunk *et al.,* 2004). It will be interesting to determine whether the differential requirement for dynamin reflects the different stimuli used to induce macropinocytosis. Are there mechanistically distinct macropinocytic pathways or might dynamin be differentially involved in the signaling pathways that lead to actin reorganization and macropinocytosis in response to these different stimuli?

A role for dynamin in cytokinesis has been shown in both *C. elegans* and *Drosophila*; however, our study provides the first direct evidence that mammalian dynamin is also required for cytokinesis. Although we cannot rule out earlier effects of the Dyn2 deficiency on cytokinesis, we observed daughter cells connected with long membrane tubules in Dyn2 KO cells and an accumulation of midbodies, suggesting a late stage defect in cytokinesis, possibly in membrane fission. Membrane fission in cytokinesis is, however, topologically distinct from membrane fission leading to vesicle release. In the latter, the dynamin collar must initiate membrane fission on the noncytoplasmic leaflet of the membrane, whereas in cytokinesis, fission must occur between cytoplasmic leaflets of the adjacent membranes. Thus, dynamin might serve other functions in cytokinesis, for example in vesicular trafficking (Albertson *et al.,* 2005). Alternatively, the role for dynamin in cytokinesis may reflect its activities in actin regulation. Interestingly, Dyn1 and -2 were functionally redundant for both cytokinesis and macropinocytosis, two actin-dependent processes. It will be important to identify dynamin mutants that uncouple these potentially distinct activities.

Finally, our in vivo reconstitution experiments are the first to analyze the functional specificity of the four Dyn2 splice variants in the absence of endogenous Dyn2. Although each has similar activities in supporting CME, our data suggests that the b variant of the first splice site within the middle domain is required for targeting Dyn2ba and Dyn2bb to the

TGN and in enabling their function in p75 export from the Golgi. The middle domain can be subdivided into a more highly conserved N-middle, mutations in which impair dynamin oligomerization (Ramachandran *et al*., 2007) and a more divergent C-middle, which bears the two Dyn2 splice regions (Schmid *et al*., 1998). These data suggest that the C-middle domain might function in intracellular targeting. Further studies will be needed to determine the mechanism by which this splice variation affects this function.

Our results differ from a previous study that suggested that the a variant of the second splice site was required for Golgi targeting (Cao *et al*., 1998). Because there is direct evidence for cell type differences in a dynamin requirement for VSV-G (vesicular stomatitis virus glycoprotein) export from the Golgi (Bonazzi *et al*., 2005), these differences may also reflect real differences between the epithelial cells used by Cao *et al*. and the fibroblastoid cells we have studied. The Dyn1 splice variant we used (Dyn1ba) was most related to Dyn2ba, and although it was targeted to the Golgi, it was not able to support p75 export from the TGN. Thus the functional distinction between Dyn1 and -2 isoforms is most likely a reflection of their different abilities to support vesicle formation (at the TGN or PM) rather than a targeting defect. Importantly, given the inability of Dyn1 to support p75 export the splice variant specificity we have observed could not be due to differential hetero-oligomer formation with endogenous Dyn1.

Our unexpected finding that Dyn2 is more effective than Dyn1 in supporting CME in nonneuronal cells and our identification of other Dyn2-specific functions coupled to the fact that Dyn2 mutants are linked to human neuropathies (Niemann *et al*., 2006) calls for more detailed functional analysis of Dyn2, a relatively understudied, yet ubiquitously expressed isoform of dynamin.

ACKNOWLEDGMENTS

We thank E. Rodriguez-Boulan, Yi Zheng (University of Cincinnati), and Peiqing Sun for plasmids and the Flow Cytometry Core and Mouse Genetics Core for technical assistance. Bill Kiosses, in the Core Microscopy Facility in TSRI helped with time-lapse microscopy. Marilyn Leonard and Suhaila White provided technical assistance in preparing the dynamin-2 targeting constructs. Shawn Ferguson and Allen Liu gave helpful suggestions. This work was supported by National Institutes of Health Grants GM42455 and MH61345 to S.L.S. and a fellowship from the National Science Council of Taiwan to Y.-W.L. This is TSRI Manuscript No. 19737.

REFERENCES

Albertson, R., Riggs, B., and Sullivan, W. (2005). Membrane traffic: a driving force in cytokinesis. Trends Cell Biol. *15*, 92–101.

Altschuler, Y., Barbas, S. M., Terlecky, L. J., Tang, K., Hardy, S., Mostov, K. E., and Schmid, S. L. (1998). Redundant and distinct functions for dynamin-1 and dynamin-2 isoforms. J. Cell Biol. *143*, 1871–1881.

Antonescu, C. N., Díaz, M., Femia, G., Planas, J. V., and Klip, A. (2008). Clathrin-dependent and independent endocytosis of glucose transporter 4 (GLUT4) in myoblasts: regulation by mitochondrial uncoupling. Traffic *9*, 1173–1190.

Artalejo, C. R., Lemmon, M. A., Schlessinger, J., and Palfrey, H. C. (1997). Specific role for the PH domain of dynamin-1 in the regulation of rapid endocytosis in adrenal chromaffin cells. EMBO J. *16*, 1565–1574.

Artalejo, C. R., Elhamdani, A., and Palfrey, H. C. (2002). Sustained stimulation shifts the mechanism of endocytosis from dynamin-1-dependent rapid endocytosis to clathrin- and dynamin-2-mediated slow endocytosis in chromaffin cells. Proc. Natl. Acad. Sci. USA *99*, 6358–6363.

Bonazzi, M. *et al*. (2005). CtBP3/BARS drives membrane fission in dynamin-independent transport pathways. Nat. Cell Biol. *7*, 570–580.

Cao, H., Chen, J., Awoniyi, M., Henley, J. R., and McNiven, M. A. (2007). Dynamin 2 mediates fluid-phase micropinocytosis in epithelial cells. J. Cell Sci.*120*, 4167–4177.

Cao, H., Garcia, F., and McNiven, M. A. (1998). Differential distribution of dynamin isoforms in mammalian cells. Mol. Biol. Cell *9*, 2595–2609.

Chen, M. S., Obar, R. A., Schroeder, C. C., Austin, T. W., Poodry, C. A., Wadsworth, S. C., and Vallee, R. B. (1991). Multiple forms of dynamin are encoded by shibire, a *Drosophila* gene involved in endocytosis. Nature *351*, 583–586.

Conner, D. A. (2001). Mouse embryonic stem (ES) cell culture. Curr. Protoc. Mol. Biol. *4*, Chapter 23, 23.3.1–23.3.6.

Conner, S. D., and Schmid, S. L. (2003). Regulated portals of entry into the cell. Nature *422*, 37–44.

Cousin, M. A., and Robinson, P. J. (2001). The dephosphins: dephosphorylation by calcineurin triggers synaptic vesicle endocytosis. Trends Neurosci. *24*, 659–665.

Damke, H., Baba, T., Warnock, D. E., and Schmid, S. L. (1994). Induction of mutant dynamin specifically blocks endocytic coated vesicle formation. J. Cell Biol. *127*, 915–934.

Ferguson, S. M. *et al*. (2007). A selective activity-dependent requirement for dynamin 1 in synaptic vesicle endocytosis. Science *316*, 570–574.

Fish, K. N., Schmid, S. L., and Damke, H. (2000). Evidence that dynamin-2 functions as a signal-transducing GTPase. J. Cell Biol. *150*, 145–154.

Gold, E. S., Underhill, D. M., Morrissette, N. S., Guo, J., McNiven, M. A., and Aderem, A. (1999). Dynamin 2 is required for phagocytosis in macrophages. J. Exp. Med. *190*, 1849–1856.

Guo, F., and Zheng, Y. (2004). Rho family GTPases cooperate with p53 deletion to promote primary mouse embryonic fibroblast cell invasion. Oncogene *23*, 5577–5585.

Henley, J. R., Krueger, E. W., Oswald, B. J., and McNiven, M. A. (1998). Dynamin-mediated internalization of caveolae. J. Cell Biol. *141*, 85–99.

Hinshaw, J. E. (2000). Dynamin and its role in membrane fission. Annu. Rev. Cell Dev. Biol. *16*, 483–519.

Hinshaw, J. E., and Schmid, S. L. (1995). Dynamin self-assembles into rings suggesting a mechanism for coated vesicle budding. Nature *374*, 190–192.

Itoh, T., Erdmann, K. S., Roux, A., Habermann, B., Werner, H., and De Camilli, P. (2005). Dynamin and the actin cytoskeleton cooperatively regulate plasma membrane invagination by BAR and F-BAR proteins. Dev. Cell *9*, 791–804.

Jones, S. M., Howell, K. E., Henley, J. R., Cao, H., and McNiven, M. A. (1998). Role of dynamin in the formation of transport vesicles from the trans-Golgi network. Science *279*, 573–577.

Kasai, K., Shin, H. W., Shinotsuka, C., Murakami, K., and Nakayama, K. (1999). Dynamin II is involved in endocytosis but not in the formation of transport vesicles from the trans-Golgi network. J. Biochem. *125*, 780–789.

Kirkham, M., Fujita, A., Chadda, R., Nixon, S. J., Kurzchalia, T. V., Sharma, D. K., Pagano, R. E., Hancock, J. F., Mayor, S., and Parton, R. G. (2005). Ultrastructural identification of uncoated caveolin-independent early endocytic vehicles. J. Cell Biol. *168*, 465–476.

Koenig, J. H., and Ikeda, K. (1989). Disappearance and reformation of synaptic vesicle membrane upon transmitter release observed under reversible blockage of membrane retrieval. J. Neurosci. *9*, 3844–3860.

Konopka, C. A., Schleede, J. B., Skop, A. R., and Bednarek, S. Y. (2006). Dynamin and cytokinesis. Traffic *7*, 239–247.

Kreitzer, G., Marmorstein, A., Okamoto, P., Vallee, R., and Rodriguez-Boulan, E. (2000). Kinesin and dynamin are required for post-Golgi transport of a plasma-membrane protein. Nat. Cell Biol. *2*, 125–127.

Kruchten, A. E., and McNiven, M. A. (2006). Dynamin as a mover and pincher during cell migration and invasion. J. Cell Sci. *119*, 1683–1690.

Krueger, E. W., Orth, J. D., Cao, H., and McNiven, M. A. (2003). A dynamin-cortactin-Arp2/3 complex mediates actin reorganization in growth factor-stimulated cells. Mol. Biol. Cell *14*, 1085–1096.

Lamaze, C., Dujeancourt, A., Baba, T., Lo, C. G., Benmerah, A., and Dautry-Varsat, A. (2001). Interleukin 2 receptors and detergent-resistant membrane domains define a clathrin-independent endocytic pathway. Mol. Cell *7*, 661–671.

Lin, H. C., Barylko, B., Achiriloaie, M., and Albanesi, J. P. (1997). Phosphatidylinositol (4,5)-bisphosphate-dependent activation of dynamins I and II lacking the proline/arginine-rich domains. J. Biol. Chem. *272*, 25999–26004.

McNiven, M. A., Cao, H., Pitts, K. R., and Yoon, Y. (2000). The dynamin family of mechanoenzymes: pinching in new places. Trends Biochem. Sci. *25*, 115–120.

Meier, O., Boucke, K., Hammer, S. V., Keller, S., Stidwill, R. P., Hemmi, S., and Greber, U. F. (2002). Adenovirus triggers macropinocytosis and endosomal

leakage together with its clathrin-mediated uptake. J. Cell Biol. *158*, 1119–1131.

Mercer, J., and Helenius, A. (2008). Vaccinia virus uses macropinocytosis and apoptotic mimicry to enter host cells. Science *320*, 531–535.

Merrifield, C. J., Feldman, M. E., Wan, L., and Almers, W. (2002). Imaging actin and dynamin recruitment during invagination of single clathrin-coated pits. Nat. Cell Biol. *4*, 691–698.

Newton, A. J., Kirchhausen, T., and Murthy, V. N. (2006). Inhibition of dynamin completely blocks compensatory synaptic vesicle endocytosis. Proc. Natl. Acad. Sci. USA *103*, 17955–17960.

Niemann, A., Berger, P., and Suter, U. (2006). Pathomechanisms of mutant proteins in Charcot-Marie-Tooth disease. Neuromolecular Med. *8*, 217–242.

Oh, P., McIntosh, D. P., and Schnitzer, J. E. (1998). Dynamin at the neck of caveolae mediates their budding to form transport vesicles by GTP-driven fission from the plasma membrane of endothelium. J. Cell Biol. *141*, 101–114.

Orth, J. D., and McNiven, M. A. (2003). Dynamin at the actin-membrane interface. Curr. Opin. Cell Biol. *15*, 31–39.

Pelkmans, L., Püntener, D., and Helenius, A. (2002). Local actin polymerization and dynamin recruitment in SV40-induced internalization of caveolae. Science *296*, 535–539.

Praefcke, G. J., and McMahon, H. T. (2004). The dynamin superfamily: universal membrane tubulation and fission molecules? Nat. Rev. Mol. Cell Biol. *5*, 133–147.

Ramachandran, R., Surka, M., Chappie, J. S., Fowler, D. M., Foss, T. R., Song, B. D., and Schmid, S. L. (2007). The dynamin middle domain is critical for tetramerization and higher-order self-assembly. EMBO J. *26*, 559–566.

Rappoport, J. Z., and Simon, S. M. (2003). Real-time analysis of clathrin-mediated endocytosis during cell migration. J. Cell Sci. *1116*, 847–855.

Sabharanjak, S., Sharma, P., Parton, R. G., and Mayor, S. (2002). GPI-anchored proteins are delivered to recycling endosomes via a distinct cdc42-regulated, clathrin-independent pinocytic pathway. Dev. Cell *2*, 411–423.

Schafer, D. A. (2004). Regulating actin dynamics at membranes: a focus on dynamin. Traffic *5*, 463–469.

Schlunck, G., Damke, H., Kiosses, W. B., Rusk, N., Symons, M. H., Waterman-Storer, C. M., Schmid, S. L., and Schwartz, M. A. (2004). Modulation of Rac localization and function by dynamin. Mol. Biol. Cell *15*, 256–267.

Schmid, S. L., McNiven, M. A., and De Camilli, P. (1998). Dynamin and its partners: a progress report. Curr. Opin. Cell Biol. *10*, 504–512.

Sever, S., Damke, H., and Schmid, S. L. (2000). Garrotes, springs, ratchets, and whips: putting dynamin models to the test. Traffic *1*, 385–392.

Shpetner, H. S., and Vallee, R. B. (1989). Identification of dynamin, a novel mechanochemical enzyme that mediates interactions between microtubules. Cell *59*, 421–432.

Singh, R. D., Puri, V., Valiyaveettil, J. T., Marks, D. L., Bittman, R., and Pagano, R. E. (2003). Selective caveolin-1-dependent endocytosis of glycosphingolipids. Mol. Biol. Cell *14*, 3254–3265.

Soulet, F., Yarar, D., Leonard, M., and Schmid, S. L. (2005). SNX9 regulates dynamin assembly and is required for efficient clathrin-mediated endocytosis. Mol. Biol. Cell *16*, 1058–2067.

Soulet, F., Schmid, S. L., and Damke, H. (2006). Domain requirements for an endocytosis-independent, isoform-specific function of dynamin-2. Exp. Cell Res. *312*, 3539–3545.

Thompson, H. M., Cao, H., Chen, J., Euteneuer, U., and McNiven, M. A. (2004). Dynamin 2 binds gamma-tubulin and participates in centrosome cohesion. Nat. Cell Biol. *6*, 335–342.

Thompson, H. M., Skop, A. R., Euteneuer, U., Meyer, B. J., and McNiven, M. A. (2002). The large GTPase dynamin associates with the spindle midzone and is required for cytokinesis. Curr. Biol. *12*, 2111–2117.

Urrutia, R., Henley, J. R., Cook, T., and McNiven, M. A. (1997). The dynamins: redundant or distinct functions for an expanding family of related GTPases? Proc. Natl. Acad. Sci. USA *94*, 377–384.

van der Bliek, A. M., and Meyerowitz, E. M. (1991). Dynamin-like protein encoded by the Drosophila shibire gene associated with vesicular traffic. Nature *351*, 411–414.

van der Bliek, A. M., Redelmeier, T. E., Damke, H., Tisdale, E. J., Meyerowitz, E. M., and Schmid, S. L. (1993). Mutations in human dynamin block an intermediate stage in coated vesicle formation. J. Cell Biol. *122*, 553–563.

Warnock, D. E., Baba, T., and Schmid, S. L. (1997). Ubiquitously expressed dynamin-II has a higher intrinsic GTPase activity and a greater propensity for self-assembly than neuronal dynamin-I. Mol. Biol. Cell *8*, 2553–2562.

Yang, L., Wang, L., and Zheng, Y. (2006). Gene targeting of Cdc42 and Cdc42GAP affirms the critical involvement of Cdc42 in filopodia induction, directed migration, and proliferation in primary mouse embryonic fibroblasts. Mol. Biol. Cell *17*, 4675–4685.

Yu, X., Odera, S., Chuang, C. H., Lu, N., and Zhou, Z. (2006). *C. elegans* dynamin mediates the signaling of phagocytic receptor CED-1 for the engulfment and degradation of apoptotic cells. Dev. Cell *10*, 743–757.